SSCL-Preprint-545
SLAC-PUB-10041

Orbit Correction System for the SSC Interaction Regions*

Y. Nosochkov and F. Pilat

Superconducting Super Collider Laboratory†
2550 Beckleymeade Ave.
Dallas, TX 75237, USA

D. Ritson

SLAC, Stanford University
Stanford, CA 94309

January 1994

*Presented at the "Workshop on Orbit Correction and Analysis," December 1–3, Brookhaven, 1993.

†Operated by the Universities Research Association, Inc., for the U.S. Department of Energy under Contract No. DE-AC35-89ER40486.

Work supported in part by Department of Energy Contract DE-AC03-76SF00515

ORBIT CORRECTION SYSTEM FOR THE SSC INTERACTION REGIONS

Y. Nosochkov, F. Pilat
Superconducting Super Collider Laboratory*
2550 Beckleymeade Avenue, Dallas, TX 75237

D.M. Ritson
SLAC, Stanford University, Stanford, CA 94309

ABSTRACT

Luminosity and performance of the colliding beam machine depend on how well the orbits of the counter rotating beams are controlled in the Interaction Regions (IRs). Two main requirements for the orbit correction in the IRs are:

- Correction of the orbit perturbations caused by magnetic and alignment errors. It could be done in a similar way as in the rest of the machine (global correction).
- Provision of the specific crossing orbit conditions at the Interaction Point (IP) and continuous control on the beam positions at the IP (local correction).

In this paper we review our design of the orbit correction system for the SSC interaction regions, and discuss the principles of the local orbit correction at the IP.

1. INTRODUCTION

To provide beam-beam collisions in the modern colliding beam machines, special sections are introduced into the lattice, called Interaction Regions (IRs). Their purpose is to bring the counter rotating beams into collision in the detector region and to attain required beam parameters at the Interaction Point (IP).

As a part of the machine lattice, the IRs need correction of the closed orbit deviations caused by magnetic and alignment errors. This correction could be done in a similar way, as it is done in the rest of the machine. Thus, we identify such a correction as a global correction.

To achieve a high luminosity and a good performance of the collider, special orbit configurations are required at the IP. They are, generally, different at injection and collision conditions, and may vary in different IRs. Therefore, an independent local correction at the IP is required for each interaction region.

The need for special crossing orbit conditions at the IP is more pronounced for multi-bunch colliding beams, typically for pp-machines. Due to a small bunch-to-bunch distance and a large space for detector, a substantial number of satellite interaction points exists in the detector region. The negative effect of these unwanted collisions can be suppressed by proper separation of the beam orbits everywhere, except at the main IP.

In this paper we discuss the current design of the orbit correction system for the SSC interaction regions, with a particular emphasis on the principles of the local orbit correction at the IP. Additional information can be found in Reference 1.

The general layout of the SSC low-β IR[2] is shown in Figure 1. The optics are antisymmetric with respect to the IP. The distance from the IP to the first quadrupole is $L^* = 20.5$m. In the final focus region two beams share the same beam pipe. They are separated into different rings by use of a set of vertical dipoles. There is a

* Operated by the Universities Research Association Inc., for the U.S. Department of Energy, under contract DE-AC35-89ER40486

Secondary Focal point (SF) on each side of the IP, located 2π in phase from the IP. The quadrupoles in the tuning section are independently powered in order to provide the squeeze of the β^* at top energy.

2. REQUIREMENTS

In this section we try to identify the specific requirements for the orbit correction in the IRs at various conditions.

- MINIMIZATION OF THE ORBIT PERTURBATIONS

Standard techniques can be used to correct the closed orbit deviations in the IR, caused by magnetic and alignment errors. Such a correction normally requires a Beam Position Monitor (BPM) and a dipole corrector next to each main quadrupole. For a better orbit control, double view BPMs have been suggested everywhere in the SSC IRs.

- BEAM SEPARATION AT INJECTION

The main IR optics provides ideally identical orbits for both beams in the final focus region. With a bunch space[3] of S_b = 5m there would be about 70 head-on collision points for each bunch in this region. This would lead to an intolerably high value of the beam-beam tune shift. The simulation studies of the beam-beam interactions[4] have been done for various beam conditions. The recommendation for injection configuration was to separate transversely the two beams in the final focus region by a distance $d \approx 20\sigma$, where $\sigma(s) = \sqrt{\varepsilon\beta(s)}$ is the rms beam radius, ε is the beam emittance, and the β-function depends on the distance s from the IP. In principle, a smaller separation could be allowed at injection. However, it is feasible to achieve the above number with the correction system to be discussed later, and it provides safer conditions.

In the detector field free region, the β-function and the beam size behave as the following functions of s:

$$\beta(s) = \beta^* + s^2/\beta^*, \qquad \sigma(s) = \sigma^* \sqrt{1 + s^2/\beta^{*2}}, \tag{1}$$

where $\sigma^* = \sigma(0)$. For a low value of β^*, clearly, the beam size rapidly increases with s, and a simple parallel separation in the whole region is not efficient.

To provide a constant effective separation $d/\sigma = n$ for equal and round beams everywhere in the detector field free region, it is enough to introduce a parallel orbit separation in one plane and a crossing angle φ in the other plane. Such a case is shown in Figure 2 with the following separations in the x and y planes (which can be interchanged):

$$d_x(s) = n\sigma^* = const, \tag{2}$$

$$d_y(s) = s\varphi_y, \quad \text{where} \quad \varphi_y = n\sigma^*/\beta^* = n\sqrt{\varepsilon/\beta^*}. \tag{3}$$

The total separation in the field free region, thus, will be as follows

$$d(s) = \sqrt{d_x^2 + d_y^2} = \sqrt{n^2\sigma^{*2}(1 + s^2/\beta^{*2})} = n\sigma(s). \tag{4}$$

Substituting the SSC injection parameters into Eqns. (2) and (3), one can get the following required values for beam separation and for the crossing angle at injection energy:

$$E = 2TeV, \quad \varepsilon = 4.7 \cdot 10^{-10} m, \quad \beta^* = 7m, \quad \sigma^* = 57\mu m,$$

$$n = 20 \Rightarrow \quad d_x = 1.14mm, \qquad \varphi_y \approx 165\mu rad. \tag{5}$$

In the final focus quadrupoles, the separation between the beams is a more complex function of s, but it is still sufficient with the conditions (5) provided.

If the orbit configurations and the β^* are kept constant while accelerating the beams, then the effective separation increases proportionally to $(1/\sqrt{\varepsilon}) \propto \sqrt{p}$, where p is the beam momentum.

♦ COLLISION CROSSING CONDITIONS

At top energy, the two beams have to be brought into collision at the main IP and be separated enough everywhere else, to suppress the effect of the long range beam-beam interactions. Simply, it is achieved by producing a crossing angle at the IP in one plane. Note that the β_{peak} in the final focus quadrupoles is much higher at collision, low-β optics (9km), than at injection (670m). Thus, the beam perturbations associated with the orbit offset in these quadrupoles are substantially magnified.

The proposal for collision orbit conditions[4] is to provide a crossing angle at the main IP with a separation at the satellite interaction points of $d \approx 14\sigma$. Since the $\beta^* = 0.5$m at collision is very small, then the beam size is almost a linear function of s ($s >> \beta^*$) in the field free region. Therefore, the same formula (3) can be used to determine the value of the crossing angle. The substitution of the appropriate collision parameters leads to the following value of φ:

$$E = 20TeV, \quad \varepsilon = 4.7 \cdot 10^{-11}m, \quad \beta^* = 0.5m, \quad \sigma^* = 4.8\mu m,$$
$$n = 14 \Rightarrow \quad \varphi \approx 135\mu rad. \tag{6}$$

The actual crossing orbits in the final focus region are shown in Figure 3. Because of opposite directions the pp-beams experience opposite focusing polarities in the common quadrupoles.

♦ LOCAL CORRECTION OF THE ORBIT

At crossing conditions the beams go off center through the final focus quadrupoles (maximum of 5.6mm at injection and 4.6mm at collision). In order to preserve the closed orbit in the rest of the machine, the beams, coming out from the triplets, must be brought back on the reference orbit by use of a set of local correction dipoles.

♦ LOCAL CORRECTION OF ANOMALOUS DISPERSION

Due to the displacements of the crossing orbits in the quadrupoles, these magnets act as well as dipoles and generate an anomalous dispersion. At collision conditions the main effect is produced by the high-β_{peak} final focus quadrupoles, where the orbit offset is a maximum. With the crossing angle of 135μrad in only one IR, the anomalous dispersion is up to 20% of the nominal dispersion in the Collider arcs and up to 10mm at the IPs. It should be cancelled at the IPs locally.

♦ COMPENSATION OF TUNING QUADRUPOLES MISALIGNMENT

In order to provide the squeeze of the β^*, the variable gradients in the IR tuning quadrupoles are changed at the top energy[2] (up to the half of the magnitude). The effect of misalignment in these quadrupoles on the closed orbit and dispersion varies along with the change of their gradients. The dipole correctors located primarily next to these quadrupoles have to compensate for this effect.

♦ CONTROL OF THE BEAM OFFSET AT THE IP

The positions of two beams at the IP may vary during collision time because of different effects, such as ground motion, current ripple, etc. A continuous orbit control at the IP and compensation of the beam-to-beam offset must be provided. For equal and round beams the geometrical reduction of luminosity due to the beam offset d^* is as follows:

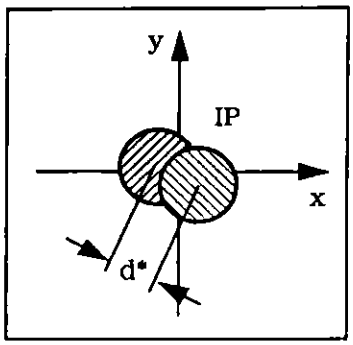

$$L/L_0 \approx exp(-d^{*2}/4\sigma^{*2}). \quad (7)$$

Therefore, for a luminosity reduction of less than 5% one can get the offset tolerance $d^* \leq 0.45\sigma^*$.

For $\sigma^* = 4.8\mu m$ this would require $d^* \leq 2.2\mu m$.

Clearly, a micron level of the orbit monitoring and orbit adjustment at the IP is required. Possible systems:

a) Continuous luminosity monitoring at the IP;

b) Local feedback orbit correction system.

3. PRINCIPLES OF LOCAL ORBIT CORRECTION AT THE IP

Our goal is to provide specific values of the orbit slope and displacement at the IP by generating a local orbit bump. To meet two conditions at the IP and to bring the beam back on the reference orbit on the other side of the IP, one needs, generally, four correction dipoles per plane (x or y). Our strategy is to use two independent pairs of dipole correctors (per plane), which are shown schematically in Figure 4:

- 1st pair: two correctors K1 and K2 are placed 2π apart from the IP on either side of the IR (SF locations) to generate the orbit slope at the IP without affecting its position.
- 2nd pair: two correctors K3 and K4 are placed $\pi/2$ away from the IP on either side of the IR to produce a displacement at the IP with no contribution to the orbit slope.

In the real design, however, the above correctors are located only approximately at the ideal phase positions. Thus, a slight coupling exists between the two pairs.

♦ CROSSING ANGLE

The crossing angle φ can be obtained by producing of the same value but opposite sign orbit slopes for two beams at the IP. Symmetrical orbit configuration leads to a minimum beam offset in the final focus quadrupoles.

Let us first remind that the effect of a single correction dipole is to generate a wave of the orbit deviation

$$x(s) = \theta\sqrt{\beta(s)\beta_\theta}\sin[\mu(s) - \mu_\theta], \quad (8)$$

$$x'(s) = \theta\sqrt{\beta_\theta/\beta(s)}\{\cos[\mu(s) - \mu_\theta] - \alpha(s)\sin[\mu(s) - \mu_\theta]\}. \quad (9)$$

where x and x' are orbit deflection and the slope, α, β, μ are the standard twiss parameters, θ is the angle kick, which is also used to indicate the twiss functions at corrector location.

It is clear from (8) and (9) that a closed orbit bump and an orbit slope at the IP can be created with the following strengths of K1 and K2 correctors:

$$x(IP) = 0, \quad x'(IP) = \varphi/2 = \theta_1\sqrt{\beta_1/\beta^*}, \quad \theta_2 = -\theta_1\sqrt{\beta_1/\beta_2}. \quad (10)$$

♦ TRANSVERSE IP DISPLACEMENT

The second pair of dipoles (K3, K4) with the following corrector strengths produce a closed orbit bump and a non-zero orbit displacement at the IP:

$$x(IP) = \theta_3\sqrt{\beta_3\beta^*}, \quad x'(IP) = 0, \quad \theta_4 = \theta_3\sqrt{\beta_3/\beta_4} \tag{11}$$

with $\alpha^* = 0$ at the IP. Such a correction can provide for:

- Beam separation at the IP by creating opposite beam displacements.
- Adjustment of IP position by equal displacement of the beam orbits.
- Correction of the beam-to-beam offset at the IP by scanning the beams with respect to each other.

♦ LONGITUDINAL IP DISPLACEMENT

The longitudinal position of the IP at crossing conditions can be adjusted by the same value but opposite sign transverse displacements of the beam orbits at the IP in the plane of crossing. This is shown in Figure 5. The longitudinal IP shift Δs linearly depends on Δx as

$$\Delta s = 2\Delta x/\varphi, \quad \text{for } \varphi << 1. \tag{12}$$

For instance for $\varphi = 135\mu$rad, a transverse displacement $\Delta x = 67.5\mu$m of each beam is required to shift the IP by $\Delta s = 1$m.

4. LOCAL CORRECTION OF THE ANOMALOUS DISPERSION

At collision crossing conditions, the main contribution to the anomalous dispersion is produced by the final focus quadrupoles with the largest orbit offset and the highest β_{peak}. Two triplets on either side of the IP amplify each other because of π phase advance between them and opposite orbit displacements. Horizontal dispersion $\Delta\eta_x$ generated by a horizontal orbit offset Δx in a quadrupole is the following function of s:

$$\Delta\eta_x(s) = \Delta x\sqrt{\beta_x(s)\beta_{qx}}(B'L_q/B\rho)\sin[\mu_x(s) - \mu_{qx}], \tag{13}$$

and similarly for y-plane, where B' and L_q are the gradient and the length of a quadrupole, and $B\rho$ is the magnetic rigidity.

At injection optics, because of modest β-functions in the final focus triplets, the anomalous dispersion is substantially smaller than at collision conditions.

The first option of dispersion correction is to use an additional set of dipole correctors. However, these dipoles, besides providing dispersion compensation, generate orbit perturbations which must be corrected as well. In practice, such a system requires rather strong correctors and produces large orbit deflections other than those in the final focus triplets.[5]

The second option, which has been chosen, is to use a set of quadrupole correctors placed in the outside dispersive regions to compensate the horizontal anomalous dispersion. A set of skew quadrupoles is required to correct the vertical dispersion. Such a system affects the dispersion directly, with no effect on the orbit. A variety of crossing conditions is allowed with modest corrector strengths.

The principle idea of dispersion correction is shown in Figure 6. The first pair of quadrupoles are placed in the dispersive region (90° FODO cells), preceding the IR, $n\pi$ apart from the first triplet. Such phase advance is available because of the specific choice of phase advance across the IR.[2] The quadrupoles are located next to main F quadrupoles, π apart from each other. They have the same β-functions, equal strengths but opposite polarities. Therefore, neither tune shift nor betatron reso-

nances are induced. The only significant effect is a wave of dispersion $\Delta\eta_{cor}$ which is proportional to the nominal horizontal dispersion $\eta_{cor,x}$ at corrector location. The effect from a single quadrupole is given by the following:

$$\Delta\eta_{cor}(s) = -\eta_{cor,x}\sqrt{\beta(s)\beta_{cor}}(B'_{cor}L_{cor}/B\rho)\sin[\mu(s)-\mu_{cor}]. \qquad (14)$$

With the same sign of nominal horizontal dispersion at both correctors, they amplify the effect of each other. With the correct strengths and polarities, the first pair of quadrupoles generate a dispersion wave which cancels the anomalous dispersion produced by the first triplet and, thus, suppress the dispersion at the IP.

The triplet on the other side of IP produces another wave of anomalous dispersion which is to be cancelled by the second pair of quadrupoles located in the dispersive region on the other side of the IP. This pair is placed $m\pi$ apart from the second triplet and is arranged in a similar way as the first quadrupole pair.

With the ideal phase advances shown in Figure 6, two pairs of correctors per each IR and per plane is enough for accurate correction with the crossing angle configuration. If the separation configuration is used instead of the crossing angle, then a small residual dispersion (<7cm) may exist in the machine due to contribution from the quadrupoles other than triplets. The complete correction can be provided with the third pair of quadrupoles placed $\pi/2$ apart from the first two pairs. This additional pair would be necessary as well, if the phase positions of correctors are not ideal.

An identical scheme is to be used to correct the anomalous vertical dispersion. In this case, the pairs of skew quadrupoles are located next to main D quadrupoles in the outside regions. The correcting vertical dispersion is proportional to the nominal horizontal dispersion at corrector locations.

The proposed system could be used not only to correct the dispersion generated in the IR, but also to compensate locally the dispersion coming into IR due to errors in the arcs. Up to 2m of the dispersion in the triplets could be corrected at collision.

5. LAYOUT OF THE CORRECTION SYSTEM

The schematic layout of the orbit correction system in the half IR is shown in Figure 7. Global correctors and BPMs are placed next to main quadrupoles. Local correctors provide the crossing conditions at the IP and are located at special positions, described in the previous sections. The other half IR is similarly arranged. For the first approximation, we assumed two dipole correctors (H and V) are next to each triplet quadrupole. However, this region is more complicated because the correction must be done for both beams simultaneously, and the phase advance is almost constant across the triplet. Further study is required for this region. All quadrupole and skew quadrupole correctors are located in the outside 90° FODO cells.

An example of the crossing angle configuration for one beam with corrected dispersion is shown in Figure 8. The maximum values of crossing angles from 175μrad to 275μrad are feasible in different IRs at collision. The case of beam separation at injection is presented in Figure 9, where the orbit displacement at the IP for one beam is shown. The maximum achievable separation at the IP is 30σ at injection. Large IP displacements (a few millimeters at collision) are possible with the simultaneous displacement of the final focus triplets.

6. ACKNOWLEDGEMENTS

We thank R. Stiening for guiding this work, his encouragement and numerous discussions, and G. Bourianoff for support and discussions.

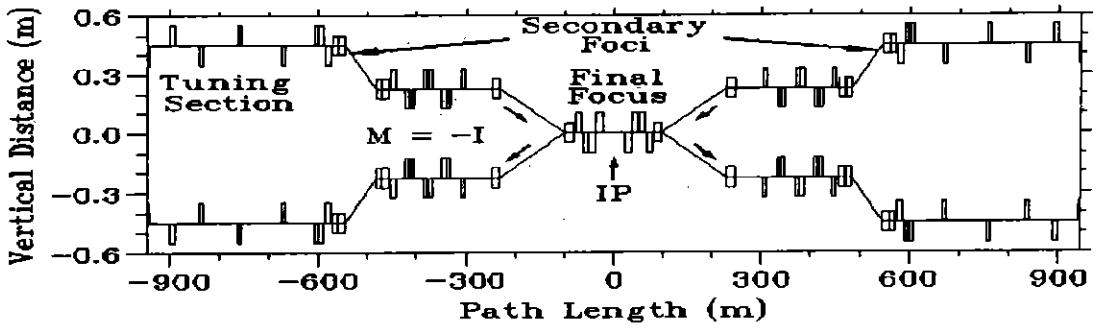

Figure 1. Vertical Layout of the SSC Low-β IR.

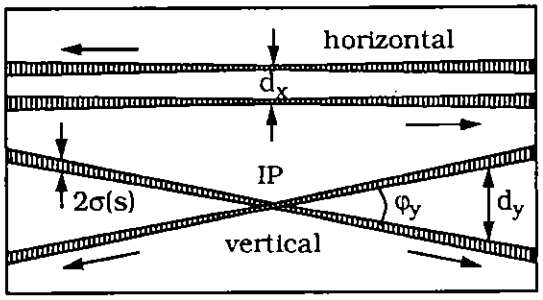

Figure 2. Separation Configuration at Injection.

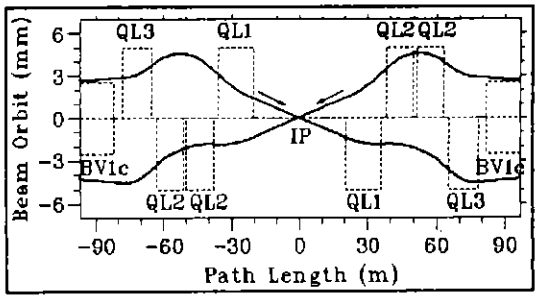

Figure 3. Collision Crossing Orbits in the Final Focus Region. φ = 135μrad.

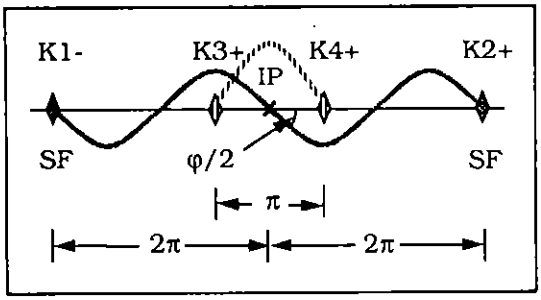

Figure 4. Principle Scheme of Local Orbit Correction at an IP.

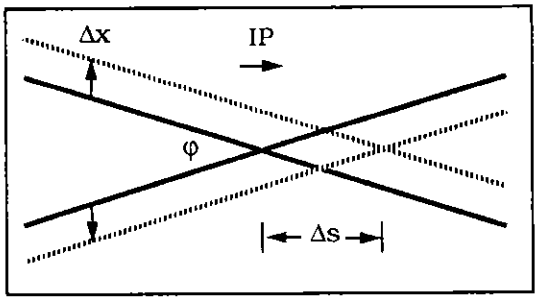

Figure 5. Longitudinal IP Displacement.

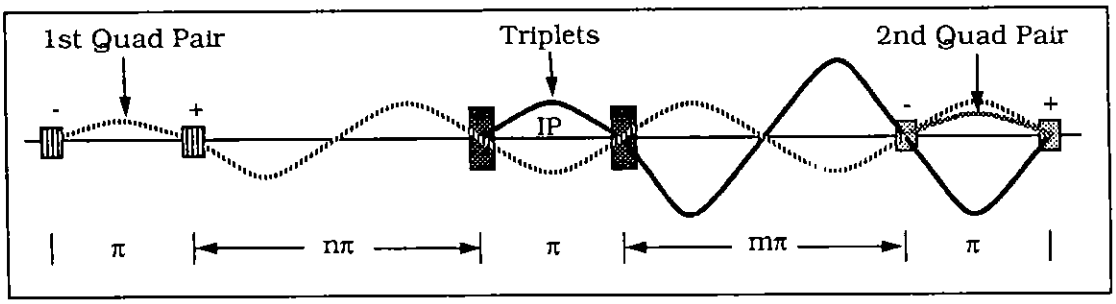

Figure 6. Principle Scheme of Local Dispersion Correction.

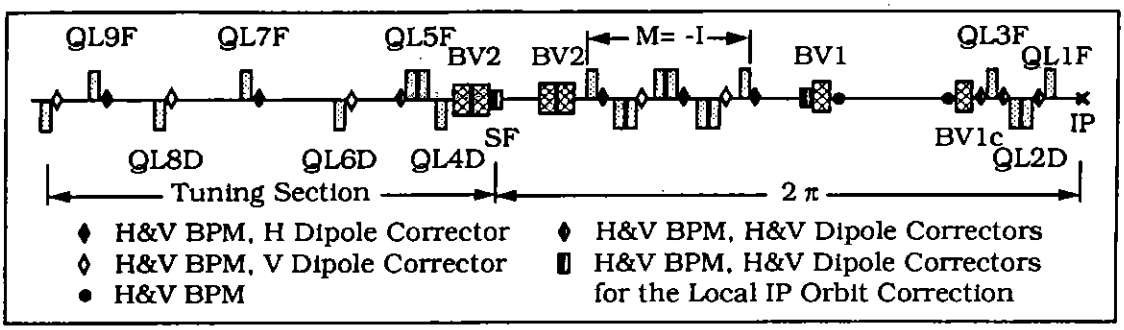

Figure 7. Distribution of Dipole Correctors in the Half IR.

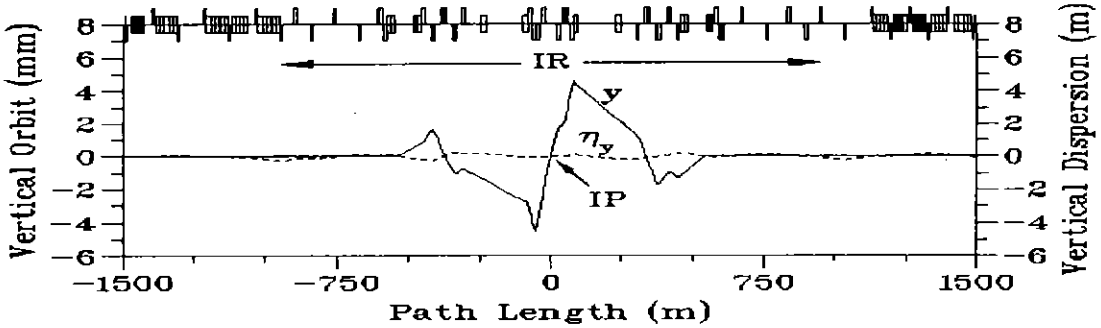

Figure 8. Beam Vertical Orbit at Collision Crossing Configuration. $\beta^* = 0.5$m.

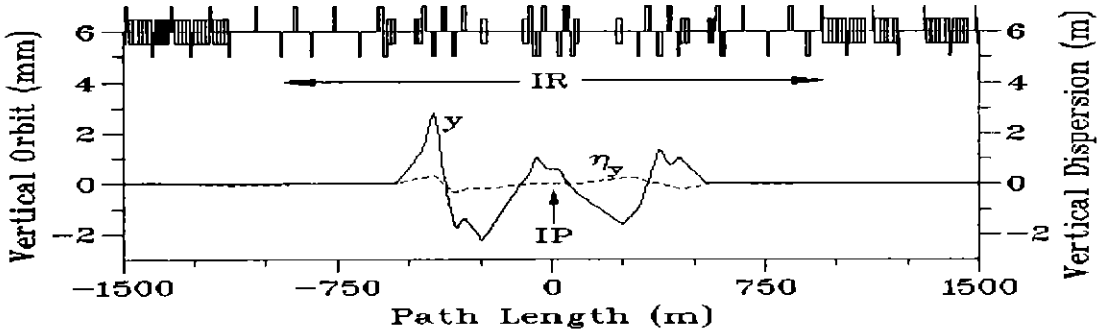

Figure 9. Beam Vertical Displacement at the IP at Injection. $\beta^* = 7$m.

7. REFERENCES

1. Y. Nosochkov and D. Ritson, "The Provision of IP Crossing Angles for the SSC," SSCL-Preprint-367, May 1993; Presented at *1993 IEEE Part. Acc. Conf.*, Washington, May 17-20, 1993.
2. Y. Nosochkov et al., "Current Design of the SSC Interaction Regions," SSCL-Preprint-368, May 1993; Presented at *1993 IEEE Part. Acc. Conf.*, Washington, May 17-20, 1993.
3. J.R. Sanford, D.M. Matthews, Eds., *Site-Specific Conceptual Design*, SSCL Document SSCL-SR-1056, 1990.
4. R. Stiening and D. Ritson, private communication.
5. A.A. Garren and D.E. Johnson, "Controlling the Crossing Angle in the SSC", In *Proc. of 1989 IEEE Part. Acc. Conf.*, Vol. 2, p. 1334, Chicago, 1989.